

Magnetic and magnetoresistive properties of inhomogeneous magnetic dual-layer films

John O. Oti, Stephen E. Russek, and Steven C. Sanders

Electromagnetic Technology Division, National Institute of Standards and Technology, Boulder, Colorado 80303

Magnetic and magnetoresistive properties of sputtered Co alloy dual-layer films are compared with micromagnetic simulations. The simulations elucidate the details of the switching behavior of the dual-layer films as a function of the interlayer exchange and magnetostatic interactions. The simulations have led to a conceptual understanding of the coercive field splitting caused by the interlayer interactions. A calculation of the anisotropic magnetoresistance (AMR) has been included in the simulations. The AMR provides a second independent macroscopic quantity (in addition to the average magnetization) which can be measured and compared with the micromagnetic simulations. The AMR is more sensitive to the micromagnetic structure perpendicular to the applied field and is a better test of the accuracy of the micromagnetic model. The simulations qualitatively describe the measured AMR data on CoNi-Cr-CoNi dual layers.

INTRODUCTION

Magnetic multilayer thin films are becoming increasingly important in the development of high coercivity media¹ and low coercivity magnetic sensors.² Magnetic interactions within and between the layers of multilayer magnetic films play an important role in determining the properties of these films.³ In this article we use our micromagnetic model^{4,5} to analyze the micromagnetics of coercive field splitting (CFS) of the major hysteresis loops and introduce magnetoresistance calculations as a tool to provide further verification of the micromagnetic model. The results of the model simulations are compared with experimental data on sputtered Co_{0.75}Ni_{0.25}-Cr-Co_{0.75}Ni_{0.25} dual-layer films.

In the micromagnetic model each magnetic layer is simulated by a rectangular array of discrete parallelepiped elements representing the grains of the layers. Each grain has a fixed magnitude magnetic moment which is allowed to dynamically relax (in three dimensions) in the presence of an external field, an effective exchange field, an effective anisotropy field, and a magnetostatic field. The magnetic layers are characterized by distributions of exchange, anisotropy, and magnetostatic parameters among the grains. The distribution of interlayer exchange coupling parameters, intralayer exchange coupling parameters, and magnetostatic interaction parameters are specified relative to certain mean values denoted, respectively, by $\langle C_e' \rangle$, $\langle C_e \rangle$, and $\langle C_{eh} \rangle$.⁶ The parameters that are assigned to the grains are selected at random from an interval centered about the mean values. Ferromagnetic interlayer exchange coupling is simulated using positive interlayer exchange parameters, and antiferromagnetic interlayer exchange coupling is simulated using negative parameters.

The films discussed in this paper are ones with moderate intragranular exchange, strong uniaxial anisotropy, and strong disorder. The disorder in these films (principally the random distribution of anisotropy axes) acts to reduce the coercive field by providing nucleation centers for the magnetization reversal. One of the most prominent features of dual-layer magnetic thin films of this type is a splitting in the coercive fields as the two layers are brought together and

allowed to interact through magnetostatic forces. At large separations, two statistically identical films will switch at approximately the same coercive field. As the films are brought closer, one film will switch first, as seen in the calculated and experimental $M-H$ curves shown in Figs. 1(a) and 1(c). We define the coercive field splitting as the difference between the top and bottom layer switching fields as determined by the distance between the peaks in the derivatives in the $M-H$ curves. The mechanism for CFS will be described in the next section.

The anisotropic magnetoresistance (AMR) can be simply modeled by assuming that each element has a change in resistance determined by the orientation of the magnetic moment relative to the current.⁷ The normalized sheet resistance of the sample is

$$R_{AMR} \approx \left[\sum_{j, \text{par}} \left(\sum_{i, \text{ser}} 1 + \delta r_{AMR} (\hat{m}_{i,j} \cdot \hat{J})^2 \right)^{-1} \right]^{-1},$$

where $\hat{m}_{i,j}$ is a unit vector along the magnetic moment of the i, j th element, \hat{J} is the direction of the current density, and δr_{AMR} is the normalized size of the anisotropic magnetoresistance. The inner summation sums the serial resistances in the direction of the current, and the outer summation sums them, reciprocally, transverse to the current. This formula does not include the effects of current redistribution and is appropriate only for systems, such as those discussed in this paper, in which the AMR is small. The average magnetization \mathbf{M} and the AMR form a set of two independent macroscopic quantities which can be computed from the micromagnetic model and compared to experimental data. Examples of computed and measured AMR for a CoNi dual-layer film are shown in Figs. 1(b) and 1(d). The AMR is quadratic in \mathbf{M} and measures the magnitude of the projection of \mathbf{M} along the current direction. In particular the AMR can probe the degree of magnetization perpendicular to the applied field and is sensitive to the details of the magnetization reversal such as the formation of vortices.

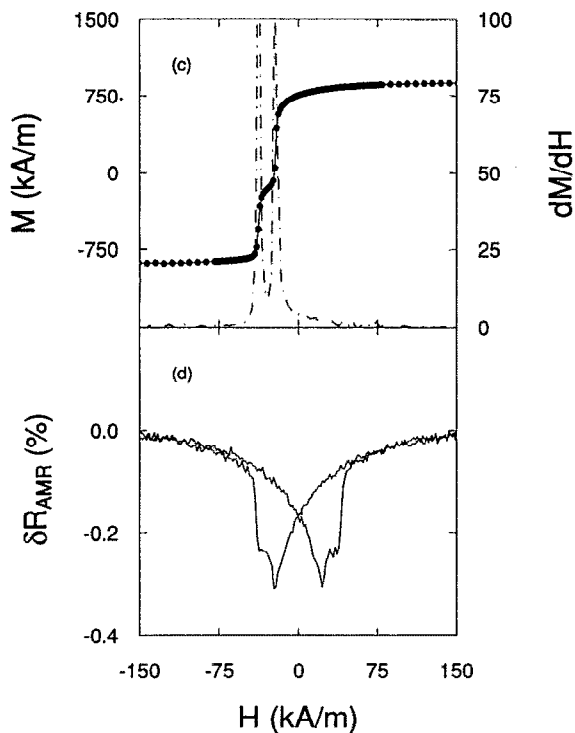
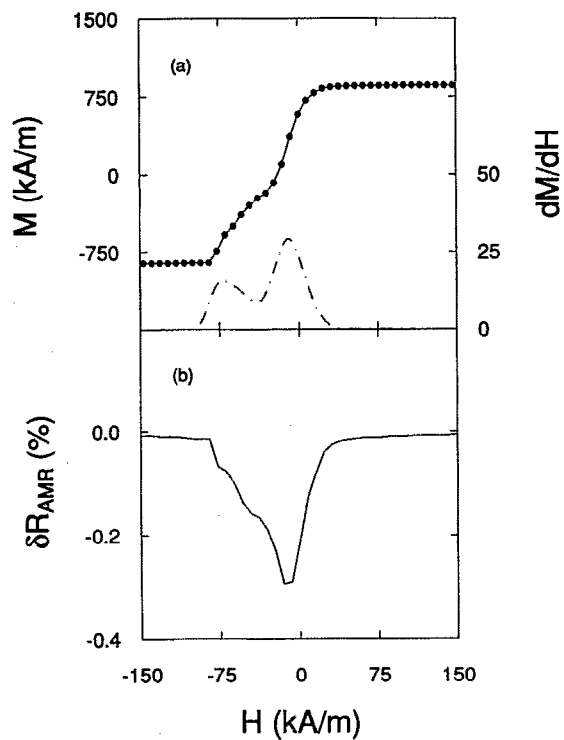


FIG. 1. (a) Calculated $M-H$ data of CoNi dual-layer film with an 8 nm Cr separation layer showing coercive field splitting (CFS). The CFS is equal to the distance between the peaks of the derivative of the magnetization (dotted curve). (b) Calculated AMR with \mathbf{H} parallel to \mathbf{J} for the same film. (c) Measured $M-H$ data for CoNi dual-layer film with 5 nm Cr separation layer showing CFS. The derivative of the magnetization is shown in the dotted curve. (d) Measured AMR with \mathbf{H} parallel to \mathbf{J} for the same film. Note that for clarity only one branch of the hysteresis loops are shown except for (d) which shows the full loop.

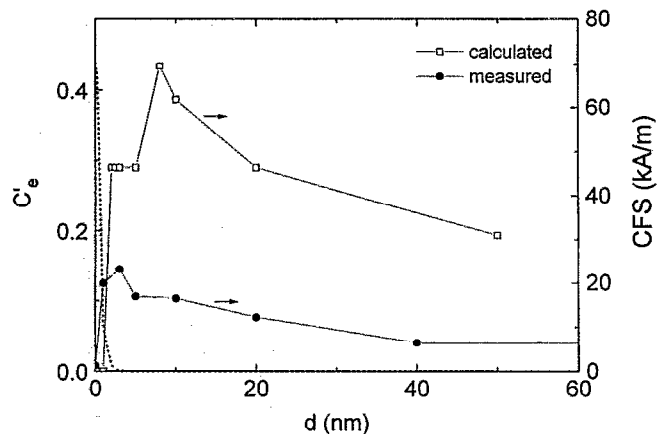


FIG. 2. Calculated and measured coercive force splitting as a function of interlayer separation d . The dotted curve on the left of the diagram represents the variation of C_e' with d .

SIMULATION AND EXPERIMENT

$\text{Co}_{0.75}\text{Ni}_{0.25}-\text{Cr}-\text{Co}_{0.75}\text{Ni}_{0.25}$ dual-layer films were sputter-deposited onto silicon substrates. The magnetic layers were each 30-nm thick, and the Cr layer thickness was varied from 1 to 80 nm. Details of the film preparation and the film microstructure are described in Ref. 4. The magnetic films are simulated by assuming a random distribution of the magnetic anisotropy axes with a uniaxial anisotropy field of $H_k=193$ kA/m (2420 Oe) and a median grain size of 22 nm. In Ref. 4, an array of 20×20 closely packed elements was used in simulating each magnetic layer of the sample. We have repeated the calculations using an array size of 50×50 elements. Periodic boundary conditions are used in the calculations to simulate the large experimental samples which have dimensions of 6×12 mm. The interlayer exchange coupling is a short-range interaction and drops off rapidly with increasing Cr spacing-layer thickness. We adopt a positive exchange constant (ferromagnetic coupling) with an exponentially decreasing form $\langle C_e' \rangle = 0.43 \exp(-2.0d)$, where d is the Cr spacing-layer thickness in nanometers. The dependence of the exchange coupling constant on spacer-layer thickness is shown in Fig. 2 (dotted curve). The same value of C_e' equal to the mean value was assigned to all the grains.

The simulations show that the magnetization reversal modes of the CoNi films are characterized by the formation and propagation of vortices in the magnetic layers. The vortices in the two layers form at different locations and different points in the hysteresis loops because of differences in their detailed microstructure. The centers of the vortices act as nucleation sites for local magnetization reversals, allowing the magnetization reversal to proceed along a low-energy path. The number of vortices in each layer initially grows with increasing externally applied field with little displacement from their original locations. Beyond a certain critical field, the vortices become extremely mobile and quickly self-annihilate, leading to complete reversal of the magnetization.

As the magnetic films are brought together they interact predominantly magnetostatically: free charges on one film attract opposite charges on the other film. The coercive fields

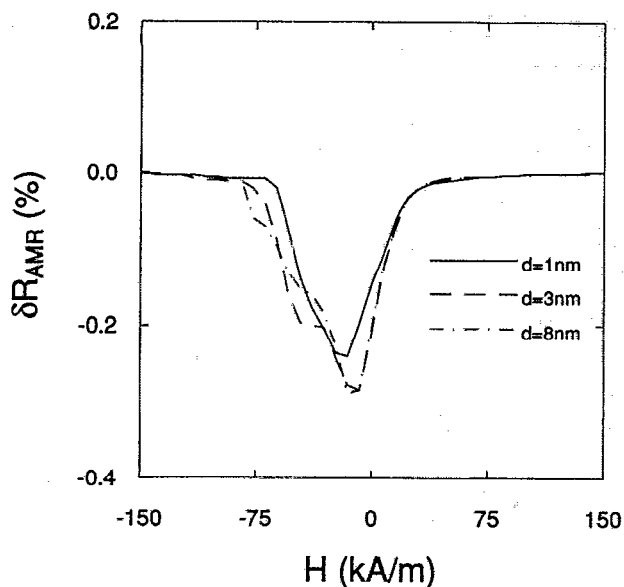


FIG. 3. Calculated AMR as a function of H for interlayer separations of 1, 3, and 8 nm (H is parallel to J).

split as shown in Figs. 1(a) and 1(c). The calculated and experimental dependence of CFS on the separation d between the magnetic layers is shown in Fig. 2. Agreement is seen in the trends of the calculated and experimental curves although magnitudes of the CFS differ. The magnitude of the CFS increases as the layers are brought together and the magnetostatic interaction increases. When the layers are sufficiently close that the exchange coupling dominates, the layers' moments are locked together and the CFS rapidly disappears.

The simulated AMR with H parallel to J is shown in Fig. 3 for different separations. The size of the AMR is directly related to the amount of magnetization perpendicular to the applied field. For smaller spacings, when the exchange interaction becomes important, the size of the AMR decreases because the layer that switches first, forces the other layer to have better registry and not have its moments lie outside the field direction.

DISCUSSION

The origin of the CFS can be understood by noting that the interlayer magnetostatic energy is a minimum in the disordered state when one of the layers has just switched and the other layer is about to switch. In this state, the disordered distribution of charges on one layer effectively compensate the disordered distribution of charges on the other layer. This magnetostatic energy minimum leads to the observed CFS, which consists of an extended stable region in which only one film has switched. An alternative approach to under-

standing the CFS is to realize that, as the layers begin to interact, they necessarily frustrate the other layer's ability to switch. When one layer begins to form a vortex in an energetically favorable location, it will cause, through the magnetostatic interaction, the other layer to reconfigure and not allow it to proceed along its lowest energy path. Therefore, when one layer switches it forces the other layer to proceed along another higher-energy path which requires a higher coercive field to switch the layer.

The coercive field splitting in the micromagnetic simulations is clearly magnetostatic in origin. The similarity of the hysteresis loops, AMR, and the dependence of the CFS on the separation layer thickness strongly suggests that the CFS seen in the experimental samples is also magnetostatic in origin. However, the interlayer exchange has not been measured in these samples, and a longer-range exchange interaction or an antiferromagnetic exchange interaction might be responsible for the observed behavior in the sputtered films. The observed splitting in the coercive fields can suggest that there is some stabilization of the antiferromagnetically aligned state and that there is antiferromagnetic exchange coupling between the layers. Often features similar to those seen in Fig. 1 have been interpreted as evidence of an antiferromagnetic exchange interaction. The results of this paper indicate that in many types of bilayer films these features can be of magnetostatic origin.

Further work needs to be done to quantify the output of the simulations (determining the correct energies and correlation functions to calculate) to obtain a better conceptual understanding of the effects of interactions in dual-layer magnetic thin films. The addition of AMR greatly improves our ability to test the accuracy of the simulations. While in the present work there is a size mismatch between the simulated sample ($1 \mu\text{m}$) and the measured sample (6 mm), this can be remedied in the future by fabricating and measuring micrometer-size samples. In this case there will be additional magnetostatic effects when the periodic boundary conditions are removed. The details of the reversal process in the range where the exchange and magnetostatic interactions are of comparable importance are still not clear, and a closer look at the micromagnetics in this range may be rewarding.

¹S. E. Lambert, J. K. Howard, and I. L. Sanders, IEEE Trans. Magn. **MAG-25**, 2706 (1990).

²R. L. White, IEEE Trans. Magn. **MAG-28**, 2482 (1992).

³J.-G. Zhu, IEEE Trans. Magn. **MAG-28**, 3267 (1992).

⁴J. O. Oti and S. E. Russek, J. Appl. Phys. **73**, 5845 (1993).

⁵J. O. Oti, IEEE Trans. Magn. **MAG-29**, 1265 (1993).

⁶Strictly speaking, six mean parameters are necessary to fully characterize a dual-layer film when the magnetic properties of the layers are different. When the properties of the layers are the same, the number of parameters reduces to three.

⁷P. Ciureanu, in *Thin Film Resistive Sensors*, edited by P. Ciureanu and S. Middelbrook (Institute of Physics, Bristol, 1992).